Rapid Large-Scale Magnetic-Field Dissipation in a Collisionless Current Sheet via Coupling between Kelvin-Helmholtz and Lower-Hybrid Drift Instabilities

I. Shinohara,[1,*] H. Suzuki,[2] M. Fujimoto,[2] and M. Hoshino[3]

[1]*Max Planck Institute for Extraterrestrial Physics, Garching 85748, Germany*
[2]*Department of Earth and Planetary Sciences, Tokyo Institute of Technology, Tokyo 152-8551, Japan*
[3]*Department of Earth and Planetary Science, University of Tokyo, Tokyo 113-0033, Japan*

(Received 29 January 2001; published 13 August 2001)

Rapid large-scale magnetic-field dissipation is observed in a full kinetic simulation of cross-field current instabilities in a current sheet even when the thickness of the current sheet is at ion scale. The Kelvin-Helmholtz instability caused by the velocity shear between the current-carrying ions and the cold background ions excites the lower-hybrid drift instability at the edges of the undulated current sheet. We show that the nonlinear coupling between these two instabilities is responsible for the observed rapid dissipation. The simulation result presents a new route for magnetic-field dissipation in an ion-scale current sheet and demonstrates the general significance of nonlinear cross-scale coupling in collisionless plasmas.

DOI: 10.1103/PhysRevLett.87.095001 PACS numbers: 52.35.Mw, 52.65.−y

Understanding cross-scale coupling between MHD and dissipation scales in collisionless plasmas is challenging. Magnetic reconnection is an impressive example of this cross-scale coupling. Although magnetic reconnection itself is a MHD scale phenomenon, its dynamics is closely related to the dissipation process in the diffusion region. Many theorists believe that the turbulence in an electron-scale current sheet or a strongly enhanced longitudinal current layer is important to provide sufficient dissipation to trigger fast reconnection in space plasmas, e.g., the magnetospheric substorm, the solar flare, etc. [1–4]. While there is observational evidence that the magnetotail current sheet thickness becomes as thin as comparable to the relevant ion inertia length prior to the substorm onset, whether it thins further down to electron scale to initiate reconnection is an open question [5]. The solar corona situation is more serious, where even the ion inertia length is much smaller than the current sheet scales [6]. Recent results of the laboratory experiments of magnetic reconnection also suggest that the thickness of the current layer is much broader than the electron inertia length [7]. It is therefore an interesting question to ask if some dissipation mechanisms set in already at ion-scale current sheets. Some among a number of instabilities associated with a current sheet can produce effective resistivity. However, no dissipation mechanism that causes the explosive onset of magnetic reconnection in an ion-scale current sheet has been reported. An aim of this work is to search dissipation processes associated with cross-field current instabilities in an ion-scale current sheet which can lead to the fast onset of magnetic reconnection. It is an important point to understand the explosive nature of magnetic reconnection which is still poorly understood [8]. In this Letter, we show a magnetic-field dissipation mechanism for an ion-scale current sheet via nonlinear coupling between the Kelvin-Helmholtz instability (KHI) [9] and the lower hybrid drift instability (LHDI) [10,11]. If a stationary background plasma is distributed outside the current sheet, the KHI caused by the shear flow between the background ions and the current-carrying ions can grow [9]. Little attention has been paid to this type of KHI because the KHI itself does not provide anomalous resistivity. However, since the KHI can significantly modulate the current sheet structure, there is a possibility that other dissipation scale instabilities, such as the LHDI, are newly excited associated with the KHI.

In order to examine the nonlinear coupling between the KHI and dissipation scale instabilities, we carry out a two-dimensional electromagnetic full kinetic simulation. For details of the scheme of our code, see Hoshino [12]. Concerning the study on cross-field current instabilities, it is known that an artificial instability called the drift kink instability (DKI) has large growth rates at a low ion-electron mass ratio $m_i/m_e < 200$ [13]. Since the DKI smears out what we expect to operate in a real plasma, the growth of the DKI must be suppressed. Note that the KHI can grow within a few tens of ion gyroperiods even for the real mass ratio, while the DKI masks the KHI in the low mass ratio regime. High capability of recent supercomputers enables us to perform full kinetic simulations with the mass ratio as large as 400 even for ion-scale phenomena as we do in this study. As the initial condition for Run 1, we make use of the Harris current sheet for simplicity; $B_z(y) = B_0 \tanh(y/D)$, $n_{cs}(y) = N_{cs}/\cosh^2(y/D)$, $J_x(y) = en_{cs}(U_i + U_e)$, and $U_i/U_e = -T_{i,cs}/T_{e,cs}$. D represents the thickness of the current sheet, which we set $D = \lambda_i$ ($\lambda_i = c/\omega_{pi}$, the ion inertia length). The simulation box size is 512 grids × 1024 grids corresponding to $8\lambda_i \times 16\lambda_i$, and $\sim 8.5 \times 10^7$ particles for both electrons and ions are used. Conducting walls are assumed at the y boundaries, $y = \pm 8\lambda_i$, while a periodic boundary condition is used for the x boundaries. In the present case, the ion-electron temperature ratio is taken to be $T_{i,cs}/T_{e,cs} = 8$ so that the ions carry most of the cross-field current. A stationary cold background plasma is distributed outside the current sheet; $n_{bk}(y) = N_{bk} \tanh^2(y/D)$, $N_{bk}/N_{cs} = 0.1$, and $T_{e,bk} = T_{i,bk} = T_{e,cs}$. (Different D and L_x are

adopted for the other three runs. See Table I.) If the cold background is uniformly introduced, the ion-ion kink instability (IIKI) [14] can grow even when the high mass ratio is taken. To avoid the growth of the IIKI, we remove the background component from around the neutral sheet. Although there appears a weak pressure imbalance with this background profile, it is quickly justified without any significant modification of the current sheet structure.

In our simulation three instabilities are excited, and each has different scale lengths; (i) the LHDI (electron scale), (ii) the current sheet kink instability (CSKI) [15] [hybrid scale, $\sim\lambda_h \equiv (\lambda_i\lambda_e)^{1/2}$], and (iii) the KHI (MHD scale). Figure 1 displays typical snapshots of each instability. First, the LHDI grows at the boundary region of the current sheet. As shown in Fig. 1a, the excited waves make electrons $\mathbf{E}\times\mathbf{B}$ drift and generate electron vortices. Since these electron vortices move in the same direction as the ion diamagnetic drift, the cross-field current in the boundary region is strongly reduced and the magnetic field is dissipated. The saturation amplitude is consistent with a previous simulation study of the LHDI [16], and the saturation is due to the electron dissipation process (details are shown later). After the saturation of the LHDI, which takes place before the appearance of the CSKI, the LHD waves are damped and the magnetic-field dissipation is much smaller than that before saturation since the cross-field current is reduced. At $t \sim 30\Omega_i^{-1}$, the neutral sheet region starts to be kinked by the CSKI (Fig. 1b). The CSKI is a drift mode driven by the cross-field current, i.e., the phase velocity is nearly equal to the ion drift velocity, and its wavelength is $k\lambda_h \sim 1$ [15]. The kink structure is generated by the perturbed electron current within the current sheet. This stage lasts until the KHI starts to evolve [$t = (30-50)\Omega_i^{-1}$] . The CSKI is presumably a short-wavelength extension of the DKI. However, the kink structure of the CSKI does not enhance the dissipation process. Finally, at $t \sim 50\Omega_i^{-1}$, the whole current sheet starts to warp with much longer wavelength $\lambda = 8\lambda_i = L_x$ (Fig. 1c). At this time, the ion flow pattern in the current sheet is globally modulated by the KHI, while it is hardly modified by the earlier two instabilities. In the KHI stage, a strong quasimonochromatic wave activity of the short wavelength appears at the edges of the undulated current sheet producing electron vortices similar to those of the LHDI at earlier time. A region of the wave activity in Fig. 1c is magnified in Fig. 2. Figure 2 clearly shows that the wave is located around the largest density gradient at the current sheet edges and is propagating along the density equicontour. To estimate the phase velocity of the wave, a stack plot of E_x at $y = 3\lambda_i$ for $t = (62-67)\Omega_i^{-1}$ is presented in Fig. 3. The phase velocity of the wave, $\sim 0.3U_i$, is about a half of the local ion drift velocity, $\sim 0.6U_i$. The electron Larmor radius in the wave region is $r_{L,e} \sim (0.2-0.3)\lambda_i$, which is comparable to the wavelength. Since all these features of the wave meet the characteristics of the LHDI [11], it is reasonable to conclude that the nonlinear evolution of the KHI excites the LHDI at the edges of the undulated current sheet. The temperature gradient in the region of wave activity is almost parallel to the density gradient (antiparallel to the magnetic-field gradient) so that the growing condition of the LHDI is satisfied. The excitation of these LHD waves continues until the KHI is saturated.

We expect that the LHDI newly activated by the nonlinear evolution of the KHI provides substantial magnetic-field dissipation since the excited LHD wave is of considerable

TABLE I. Simulation parameters and LHD amplitudes observed after the KHI growth.

Run	D/λ_i	$L_x/\lambda_i \times L_y/\lambda_i$	$c\lvert\delta E_{lhd}\rvert/B_0$	η_{eff}
1	1	8×16	~ 0.1	$1.4\times 10^{-3}\omega_{pe}^{-1}$
2	1	2×16	$\cdots$	$\cdots$
3	3/4	6×16	~ 0.15	$1.7\times 10^{-3}\omega_{pe}^{-1}$
4	1/2	4×16	~ 0.2	$2.2\times 10^{-3}\omega_{pe}^{-1}$

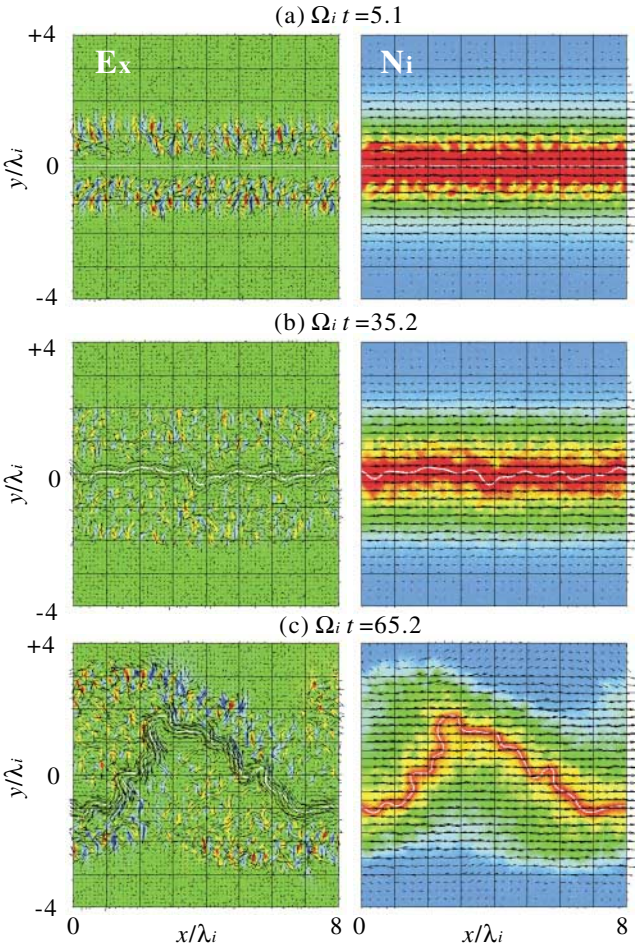

FIG. 1 (color). Left three panels present color contours of E_x, which is the dominant component of the electric field, at $t = 5.1\Omega_i^{-1}$, $35.2\Omega_i^{-1}$, and $65.2\Omega_i^{-1}$. In each contour the electron flow vectors are also plotted. Right three panels show color contours of the ion density and the ion flow vectors at the same time. The white lines represent the magnetic neutral lines.

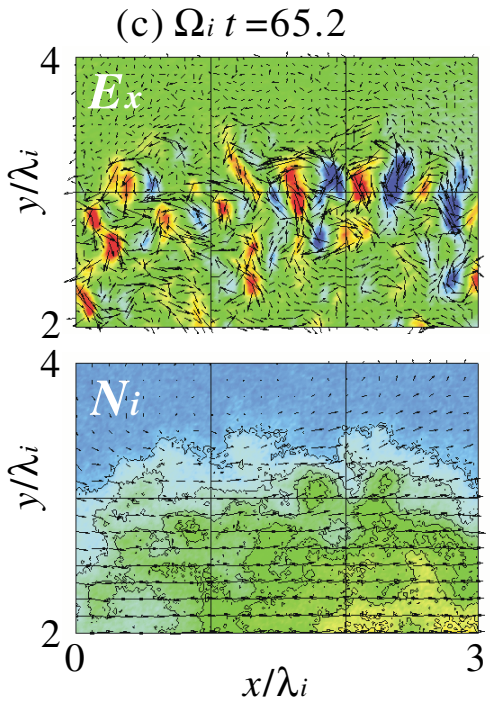

FIG. 2 (color). Magnification of Figure 1c.

amplitude and the wave activity is widely distributed. Indeed, the amplitude of the LHD wave observed in the KHI stage is almost equal to that observed in the first LHDI stage ($c|\delta E_{lhd}|/B_0 \sim 0.1$). To examine how much of the magnetic-field energy ($\equiv E_B$) is dissipated in the simulation run, the time evolution of E_B is shown in Fig. 4a. Three stages are recognized in the solid curve of Fig. 4a, and each stage corresponds to the three instability stages noted above. In the first stage, about 1% of the initial magnetic-field energy ($\equiv E_{B0}$) is lost within $10\Omega_i^{-1}$ by the LHDI. After the saturation of the LHDI, the dissipation rate (the gradient of the E_B curve) is considerably reduced for $t = (10-50)\Omega_i^{-1}$. After the KHI starts to grow,

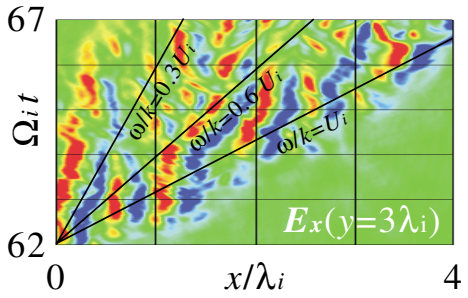

FIG. 3 (color). A stack plot of E_x at $y = 3\lambda_i$ for $t = (62-67)\Omega_i^{-1}$. The lines indicate the measure of the phase velocities.

the dissipation rate increases and a rapid magnetic-field dissipation is observed. Since the LHDI is continuously driven by the KHI, the high dissipation rate is kept during the KHI stage. As a result, about 10% of E_{B0} is dissipated within about $50\Omega_i^{-1}$. To confirm the effect of the coupling process to the dissipation, we carry out another simulation run in which the KHI is forbidden by setting $L_x = 2\lambda_i$ (Run 2 in Table I). Consistent with a linear analysis, we do not observe growth of the KHI in this run. The dashed curve in Fig. 4a presents the E_B hysteresis obtained from this case without the KHI. Rapid drop of E_B after $t = 50\Omega_i^{-1}$ cannot be found without the KHI. Figure 4a well supports our suggestion that the nonlinear coupling between the KHI and the LHDI indeed provides the substantial magnetic-field dissipation. We should note that this rapid magnetic field dissipation process may occur before magnetic reconnection starts. Indeed, the tearing instability is observed at a much later time in a two-dimensional full kinetic simulation with the same parameter if no initial perturbation (such as the driven flow from the boundaries, etc.) is added to the Harris equilibrium. However, the observed rapid dissipation process should be a transient process since the drive for the KHI comes entirely from the overlap of the cold stationary ions and the current-carrying ions. Thus, the dissipation process

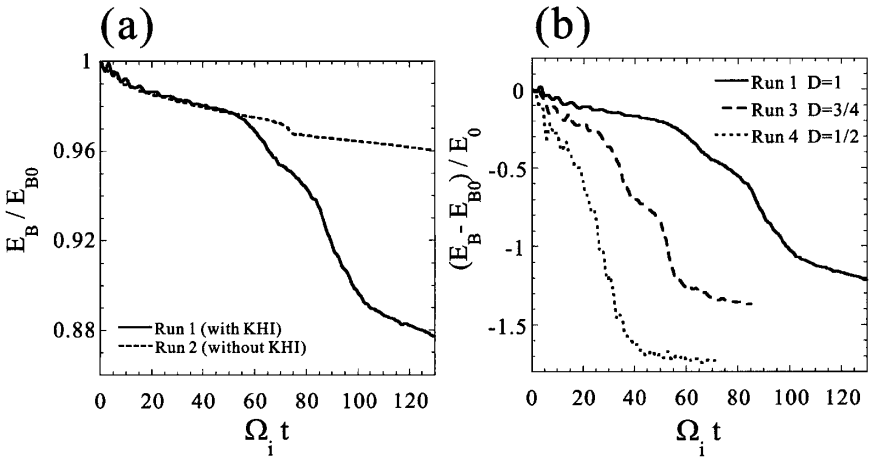

FIG. 4. (a) Solid and dashed curves represent evolution curves of E_B/E_{B0} for Run 1 (with the KHI) and 2 (without the KHI). (b) Evolution curves of $(E_B - E_{B0})/E_0$ for Run 1 (solid), 3 (dashed), and 4 (dotted).

reported here is unlikely to be observed in the steady-state reconnection.

We have also examined the effects of the current sheet thickness D (Runs 1, 3, 4 in Table I). Figure 4b presents the evolution curves of the diminution of the magnetic field energy for each run. [The magnetic-field energy is normalized by $E_0 \equiv L_x \lambda_i (B_0^2/8\pi)$.] As predicted by linear theory of the KHI [15], the start time of the KHI growth that marks the onset of rapid large-scale dissipation scales as $\sim D^2$ ($t = 15$, 34, and 60 for $D = 1/2$, 3/4, and 1). In the case of $D/\lambda_i = 1/2$, the KHI starts to grow so quickly that the CSKI stage is deleted. The LHD amplitudes in the KHI stage are shown in Table I. Similar to the result of Run 1, the typical wave amplitudes are almost equal to those observed in the first LHDI stage and the amplitude shows a dependence of $\sim D^{-1}$. This dependence is consistent with a previous study [16]. We also find that the duration of the rapid large-scale dissipation scales as $\sim D$. Since the dissipation rates observed in the first LHDI stage and the KHI stage are almost equal, the fact that the KHI continuously drives the LHDI is an important issue for the rapid large-scale magnetic dissipation. For the reader's convenience, the effective resistivity for the rapid dissipation process is also shown in Table I. The effective resistivity, $\eta_{\rm eff}$, is estimated from Ohm's law, $\langle \mathbf{E} + \mathbf{V_e} \times \mathbf{B}/\mathbf{c} \rangle = \eta_{\rm eff} \langle \mathbf{J} \rangle$. $\mathbf{E} + \mathbf{V_e} \times \mathbf{B}/\mathbf{c}$ and $\mathbf{J}$ are averaged over the entire current sheet. The estimated values are the same order with, but smaller than, that of the DKI estimated by Horiuchi *et al.* [17].

Finally, we should comment on the electric field at the magnetic neutral line. An electric field along the current at the neutral line is necessary for magnetic reconnection. As shown in Fig. 1c, however, no electric field right at the neutral can be found. What is taking place inside the current sheet is the emergence of an intense current layer that compensates the reduced current at the edges. This compensation is required from the conservation of the total current integrated over the current sheet. (The magnetic field at the y boundary is invariant as long as the perturbation from the current sheet does not reach the boundary.) The compensative current is embedded in a relatively narrow region around the neutral sheet and is carried by accelerated meandering electrons. The electron acceleration takes place at the edges of the embedded current sheet (but not at the neutral sheet) and is the very origin of the dissipation process [Shinohara *et al.* (to be published)]. While recent results of three-dimensional full kinetic simulations with a low mass ratio ($m_i/m_e < 200$) [17,18] show that reconnection can be triggered by the DKI, there is a crucial difference that the DKI can directly produce the reconnection electric field at the neutral sheet but the KHI does not. The relation between the KHI and the magnetic reconnection still needs investigation and we plan a three-dimensional simulation for this end. Since the dissipation process reported here drastically modifies the current sheet structure, even if reconnection is not driven directly by the present process, it is quite unlikely that its effects on a subsequent process leading to reconnection may be ignored. For example, the newly accelerated meandering electrons can affect the growth of the electron tearing mode. Recently, Rogers *et al.* [19] reported that the LHD fluctuations cause a substantial relaxation of the density gradient and reduce the reconnection rate. While the reconnection electric field is supported by the electron shear flow mode associated with the sharp gradient (turbulence in the electron inertia scale) in their simulation, such a sharp gradient does not appear in our model due to the LHD mode. Therefore, the mechanism that is responsible for the reconnection electric field might be different even if our model can successfully trigger magnetic reconnection.

In summary, we find a new route for magnetic-field dissipation in an ion-scale current sheet. Within several tens of ion gyroperiod, considerable magnetic-field energy is dissipated through the nonlinear coupling between the KHI and the LHDI. This dissipation time scale is so short that it may be applicable to the magnetospheric substorm onset. We believe that the process reported here is a good demonstration for the general significance of nonlinear cross-scale coupling in collisionless plasmas.

I. S. thanks Dr. M. Scholer and Dr. R. Treumann for their fruitful discussions. This work has been supported by STE Laboratory of Nagoya University via a collaborative research program. Numerical simulations are performed on Fujitsu VPP at ISAS and Nagoya University.

*Permanent address: Institute of Space and Astronautical Science, Kanagawa 229-8510, Japan.

[1] J. F. Drake *et al.,* Phys. Rev. Lett. **73**, 1251 (1994).
[2] D. Biskamp *et al.,* Phys. Rev. Lett. **76**, 1264 (1996).
[3] J. Aparicio *et al.,* Phys. Plasmas **5**, 3180 (1998).
[4] R. M. Kulsrud *et al.,* Phys. Plasmas **5**, 1599 (1998).
[5] V. A. Sergeev *et al.,* J. Geophys. Res. **95**, 3819 (1990).
[6] T. Terasawa *et al.,* Adv. Space Res. **26**, 573 (2000).
[7] M. Yamada *et al.,* Phys. Plasmas **7**, 1781 (2000).
[8] J. F. Drake, Nature (London) **410**, 525 (2001).
[9] P. H. Yoon *et al.,* J. Geophys. Res. **101**, 27 327 (1996).
[10] N. A. Krall *et al.,* Phys. Rev. A **4**, 2094 (1971).
[11] R. C. Davidson *et al.,* Phys. Fluids **20**, 301 (1977).
[12] M. Hoshino, J. Geophys. Res. **92**, 7368 (1987).
[13] W. Daughton, J. Geophys. Res. **103**, 29 429 (1998).
[14] W. Daughton, Phys. Plasmas **6**, 1329 (1999).
[15] H. Suzuki *et al.,* Adv. Space Res. (to be published).
[16] J. U. Brackbill *et al.,* Phys. Fluids **27**, 2682 (1984).
[17] R. Horiuchi *et al.,* Phys. Plasmas **6**, 4565 (1999).
[18] G. Lapenta, Nonlinear Proc. Geophys. **7**, 151 (2000).
[19] B. N. Rogers *et al.,* Geophys. Res. Lett. **27**, 3157 (2000).